N87-17953

TDA Progress Report 42-88 October–December 1986

Fixed Lag Smoothers for Carrier Phase and Frequency Tracking

R. Kumar[1] and W. J. Hurd
Communications Systems Research Section

The article presents the application of fixed lag smoothing algorithms to the problem of estimation of the phase and frequency of a sinusoidal carrier received in the presence of process noise and additive observation noise. A suboptimal structure consists of a phase-locked loop (PLL) followed by a post loop correction to the phase and frequency estimates. When the PLL is operating under a high signal-to-noise ratio, the phase detector is approximately linear, and the smoother equations then correspond to the optimal linear equations for an equivalent linear signal model. The performance of such a smoother can be predicted by linear filtering theory. However, if the PLL is operating near the threshold region of the signal to noise ratio, the phase detector cannot be assumed to be linear. Then the actual performance of the smoother can significantly differ from that predicted by linear theory. In the article we present both the theoretical and simulated performance of such smoothers derived on the basis of various models for the phase and frequency processes.

I. Introduction

The derivation of optimum receivers through modern estimation techniques has been proposed by various researchers (see Refs. 1–12 and their references). In Refs. 4 and 5 optimum zero lag receivers have been derived on the basis of linear Kalman filtering theory (Ref. 6) for linear measurement schemes. The nonlinear measurement situations which are of interest here have been studied in Ref. 7, wherein, on the basis of nonlinear filters of Ref. 8, suboptimal nonlinear zero lag receivers have been derived for the demodulation of angle modulated signals. In Ref. 9 the techniques of Refs. 7 and 8 have been extended to design suboptimum fixed lag smoothers for phase estimation. The solution of the optimum nonlinear filtering/smoothing problem is, of course, intractable. Whether derived from linear or nonlinear theory, the smoother structure consists of a phase-locked loop (PLL) followed by a post loop correction to the phase and frequency estimates.

In this article we study the application of linear and nonlinear smoothers to the phase and frequency estimation of a sinusoid. We show that for this case, the suboptimum nonlinear smoother derived from Refs. 7–9 is not substantially different from the optimum linear smoother equations for an appropriate linearized measurement model. In addition, simu-

[1] Also with the faculty of the Electrical Engineering Department at California State University, Long Beach.

lations show that the difference in performance of the nonlinear and linear smoother is not significant, even when the phase detector is operating highly nonlinearly. Even though the linear and nonlinear systems perform similarly, linear theory is inadequate to predict the performance when the phase detector is highly nonlinear.

When compared to the case of linear phase detector, the performance of the smoother for the case of nonlinear phase detector can be substantially different. The difference can be much more pronounced when process noise is present, compared to the case when only observation noise is present. The simulation examples indicate that in the absence of process noise, although there is a significant performance degradation due to nonlinearity (about 1 dB when operating in the loop SNR of about 5 dB), there is no threshold observed in the smoothing error covariance in this region. In contrast to this, there is a pronounced threshold in the smoother performance when the process noise is present and the inverse of filter phase error variance is below 7.5 dB.

We also evaluate the smoother performance when the process noise is reduced in magnitude. That is, the smoother/filter solutions are based on a relatively high process noise, but in the simulation the actual variance of the process noise used is lower or zero. This is of interest because, in many practical applications, the process noise statistics are not precisely known, and are therefore deliberately over-estimated.

II. Signal Model and Smoother Equations

In this section, we present a suboptimal nonlinear smoother, and show that it is very similar to the linear solution. We then present an implementation of the linear solution. We consider the problem of estimating the phase process $\theta(k)$ from the sampled version of the received carrier signal $y(k)$, i.e.,

$$y(k) = A\sqrt{2}\sin(\omega_c t_k + \theta(k)) + \overline{v}(k) \tag{1}$$

where t_k is the kth sampling time, ω_c is the known carrier frequency and $\overline{v}(k)$ the observation noise is the sampled version of a narrow band zero mean white Gaussian noise process $v(t)$. Furthermore, the phase process $\theta(k)$ is modeled as

$$\left.\begin{aligned} \theta(k) &= \beta \ell' x(k), \qquad \ell' = [1\ 0\ \ldots\ 0] \\ x(k+1) &= \Phi x(k) + w(k) \end{aligned}\right. \tag{2}$$

In Eq. (2), β is the phase constant, $x(k)$ is the state vector of dimension n, Φ is an $(n \times n)$ matrix and $w(k)$ is zero mean white Gaussian noise process independent of $\{\overline{v}(k)\}$. Thus

$$E[\overline{v}(k)] = 0\ ,\quad E[w(k)] = 0$$

$$E[\overline{v}^2(k)] = R\ ;\quad E[w(k)w^T(k)] = Q\ ;\quad E[\overline{v}(k)w(j)] = 0$$

As shown in Refs. 9 and 10, when $2\omega_c t$ and higher order harmonic terms are ignored, the smoother equations reduce to the following:

$$\left.\begin{aligned} \hat{x}_0(k+1) &= \Phi\hat{x}_0(k/k) + K_0(k+1)\eta(k+1) \\ \hat{x}_i(k+1/k+1) &= \hat{x}_{i-1}(k/k) + K_i(k+1)\eta(k+1) \\ \eta(k+1) &= \sqrt{2}y(k+1)\operatorname{Cos}(\hat{\Theta}(k+1)) \\ \hat{\Theta}(k+1) &= \omega_c t_{k+1} + \beta\ell'\hat{x}(k+1/k) \\ x_i(k) &\triangleq x(k-i), \qquad i = 0,\ldots,L \end{aligned}\right\} \tag{3}$$

where $\hat{x}_i(k/k)$ represents the filtered estimate of $x_i(k)$ or the smoothed estimate $\hat{x}(k-i/k)$. The gain vectors K_i and the cross covariance matrices $P_{i0}(k/j) \triangleq E\{\tilde{x}(k-i/j)\,\tilde{x}^T(k/j)\}$ with $\tilde{x}(k/j) \triangleq x(k) - \hat{x}(k/j)$ are given by

$$K_i(k+1) = A\,\beta P_{i0}(k+1/k)\,\ell\, S^{-1}(k+1)\,, \qquad 0 \leqslant i \leqslant L \tag{4}$$

$$\begin{aligned} P_{i0}(k+1/k+1) &= P_{i0}(k+1/k) \\ &\quad - P_{i0}(k+1/k)(A\beta\ell)(A\beta\ell)' \\ &\quad \times P_{00}(k+1/k)S^{-1}(k+1) \end{aligned} \tag{5a}$$

$$P_{i0}(k+1/k) = P_{i-1,0}(k/k)\,\Phi'\,, \qquad 0 < i \leqslant L \tag{5b}$$

$$\begin{aligned} S^{-1}(k+1) &= A^{-2}\left(p_\phi - \frac{1}{2}p_\phi^2\right)^{-1} \\ &\quad \times \left\{1 - \left[\frac{\tilde{R}(k+1) + p_\phi^2}{\tilde{R}(k+1) + 2p_\phi}\right]^{1/2}\right\} \\ p_\phi &= \beta^2 P_{00}^{1,1}\,, \qquad \tilde{R}(k) = R(k)/A^2 \end{aligned} \tag{6}$$

The smoother error covariance matrix $P_{ii}(k+1/k+1)$ is

$$P_{ii}(k+1/k+1) = P_{ii}(k+1/k) - P_{i0}(k+1/k)(A\beta\ell)$$

$$\times S^{-1}(k+1)(A\beta\ell)' P'_{i0}(k+1/k)$$

$$P_{ii}(k+1/k) = P_{i-1,i-1}(k/k) \tag{7}$$

A. Rapprochement With Linear Theory

Representing the bandpass additive noise $\overline{v}(k)$ in terms of its baseband quadrature components $\overline{v}_i(k)$ and $\overline{v}_q(k)$, ignoring the $2\omega_c$ term, then for small estimation error $\widetilde{x}(k+1/k)$,

$$\eta(k+1) = \beta A\ell'\widetilde{x}(k+1/k) + \frac{1}{\sqrt{2}}\overline{v}_i(k+1) \tag{8}$$

The $\eta(k+1)$ given by Eq. (8) above is precisely the one-step ahead prediction error (innovation) for the following linear model

$$y(k+1) = \beta A\ell' x(k+1) + \frac{1}{\sqrt{2}}\overline{v}_i(k+1) \tag{9}$$

It is easily verified that Eqs. (3–7) reduce to the linear optimal smoother equations for the model (Eqs. [2, 9]), under the assumption of small p_ϕ.

B. Smoother Implementation

If the various gains are replaced by their respective steady state values, the smoother consists of a digital phase-locked loop followed by a post-loop correction to the filtered estimates. As shown in Ref. 10 this post-loop correction can be equivalently implemented by a finite impulse response (FIR) filter whose output $\epsilon(k+1)$ is related to its input $\eta(k+1)$, as in Fig. 1, by

$$\epsilon(k+1) = \eta(k+1) + \gamma^{-1}\eta(k) + \ldots + \gamma^{-(L-1)}\eta(k+2-L) \tag{10}$$

The scalar γ in Eq. (10) can be expressed in terms of steady state filter error covariance matrix, etc., as shown in Ref. 10.

III. Linear Filter/Smoother: Derivation of Transfer Functions and Performance Expressions

In Ref. 10, three specific cases of model (2) are considered. These correspond to the dimension n of the state vector x in Eq. (2) equal to 1, 2, and 3. The resulting filter/smoother configurations are termed first order, second order and third order respectively. By replacing various gains and matrices by their steady-state values in Eqs. (3–7), these difference equations are replaced by algebraic equations and may be solved explicitly for the steady state values of the filter error covariance matrix P_F, the prediction error covariance P_p, smoother error covariance P_S, etc. Substitutions of these expressions in Eq. (4) and the linearized version of Eq. (6) results in the steady-state expressions for the filter and smoother gains. Finally, from Eq. (3) the filter and smoother transfer functions and various other transfer functions of interest are derived. These expressions are very useful in evaluating the error performance of the filter/smoother when the design value of the process noise covariance matrix is different than its actual value. In such cases, the expressions derived for the filter/smoother covariance matrices do not reflect the actual performance. The various error variances are instead evaluated using frequency domain techniques from the derived transfer functions. One may refer to Ref. 10 for the details of such derivations.

The above derivations are based on the assumption of linear phase detector. The performance predicted on the basis of these expressions is compared with simulations in the next section. As would be observed there, under the assumption of linear phase detector, the simulation results are in close conformity with those predicted from theory.

IV. Simulation Results

In the following the simulation results obtained for the second-order case are presented in some detail. We discuss the performance of the optimal linear filter and smoother both with linear phase detectors first. Then we evaluate the smoother performance versus delay and lastly discuss the smoother performance with the nonlinear phase detector. To be concrete we use the following often used model for the Q matrix

$$Q = \begin{bmatrix} T^2/3 & T/2 \\ T/2 & 1 \end{bmatrix} \sigma_a^2\ T^2 \tag{11}$$

One advantage of using the above Q is that the performance of the filter/smoother is then a function of only three parameters viz. σ_a, $\sigma_{\overline{v}}$, and T, where $\sigma_{\overline{v}}^2$ denotes the noise variance of $v_i(k)/\sqrt{2}$ in the baseband model, Eq. (9). We present the smoother/filter performance in terms of the phase estimation error. One may refer to Ref. 10 for the corresponding results for the frequency estimation error.

First we present the phase tracking performance from both analysis and simulations for the case when the phase detector nonlinearity is ignored. Both the optimal filter and smoother performance are analyzed in the following.

1. Optimal filter and smoother with large delay. Here we present the performance of the optimal filter and smoother (assuming linear signal model) so as to relate these parameters to the two-sided normalized loop noise bandwidth $2B_p$, a commonly used parameter in the design of phase locked loops. We consider the smoother with large delay. In terms of the closed-loop transfer function matrix $G_F(z)$ (Ref. 10), the parameter $2B_p$ is given by,

$$2B_p = \frac{1}{2\pi j} \int_\Gamma G_{F,p}(z)\, G_{F,p}(z^{-1})\, \frac{dz}{z} \qquad (12)$$

where $G_{F,p}$ represents the first component of the transfer function matrix $G_F(z)$, and Γ is some appropriate contour of integration. Figure 2 plots B_p as calculated from Eq. (12) as a function of $(\sigma_a^2/\sigma_{\bar{v}}^2)$ for three different values of the sampling period T viz. 0.01, 0.1 and 1 s. From these graphs it is readily seen that approximately,

$$\left.\begin{aligned} 2B_p &\cong 0.67\, (\sigma_a^2/\sigma_{\bar{v}}^2)^{0.11}\, T, && T = 1\text{ s}, \sigma_a^2/\sigma_{\bar{v}}^2 \leqslant 10 \\ 2B_p &\cong 1.01\, (\sigma_a^2/\sigma_{\bar{v}}^2)^{0.226}\, T, && T = 0.1\text{ s} \\ 2B_p &\cong 1.05\, (\sigma_a^2/\sigma_{\bar{v}}^2)^{0.25}\, T, && T = 0.01\text{ s} \end{aligned}\right\} \qquad (13)$$

The last relation may be taken to be the asymptotic relation for $(2B_p/T)$ as $T \to 0$. Figure 2 also includes the normalized loop noise bandwidth of the smoother as calculated from Eq. (12) with $G_{F,p}$, replaced by the first component of the smoother transfer function matrix. Denoted by $2B_{p,S}$ this normalized bandwidth is given by

$$2B_{p,S} \cong 0.28\, (\sigma_a^2/\sigma_{\bar{v}}^2)^{0.234}\, T, \qquad T = 0.1\text{ s} \qquad (14a)$$

Comparison with the filter bandwidth of Eq. (13) yields

$$B_p/B_{p,S} \cong 3.6\, (\sigma_a^2/\sigma_{\bar{v}}^2)^{-0.008}, \qquad T = 0.1\text{ s} \qquad (14b)$$

This indicates that the improvement achievable by using second order smoothing compared to a second order filter is approximately a factor of 3 · 6 or 5.5 dB.

The real two-sided noise bandwidth of the filter $2B_{Lp} = 2B_L/T$ and is equal to the normalized phase error variance $P_F(1,1)/(\sigma_{\bar{v}}^2 T)$ when the actual process variance $\sigma_{a,S}^2 = 0$. Similarly

$$2B_{Lp,S} = 2B_{p,S}/T = P_S(1,1)/(\sigma_{\bar{v}}^2 T)$$

In Fig. 3 we plot the normalized phase error variance for both the filter and smoother as obtained from the recursive solutions of Eqs. (4–7). From the figure approximate expressions for these terms may be written as,

$$\begin{aligned} P_F(1,1)/\sigma_{\bar{v}}^2 T &\cong 0.75\, (\sigma_a^2/\sigma_{\bar{v}}^2)^{0.08}, \quad T = 1\text{ s},\ \sigma_a^2/\sigma_{\bar{v}}^2 \leqslant 10 \\ &\cong 1.32\, (\sigma_a^2/\sigma_{\bar{v}}^2)^{0.22}, \quad T = 0.1\text{ s} \\ &\cong 1.4\, (\sigma_a^2/\sigma_{\bar{v}}^2)^{0.25}, \quad T = 0.01\text{ s} \end{aligned} \qquad (15a)$$

$$P_S(1,1)/(\sigma_{\bar{v}}^2 T) = 0.365\, \sigma_a^2/\sigma_{\bar{v}}^2{}^{\,0.237} \qquad (15b)$$

Comparing Eqs. (15) and (13,14) one observes that provided an optimum filter or smoother is used, the maximum degradation of the phase error variance is only about 1.34 (1.25 dB) and this is almost independent of the variance σ_a^2.

2. Optimal smoother performance with linear phase detector. In Fig. 4 is plotted the smoother performance evaluated from simulations as a function of the smoother delay and the ratio $(\sigma_a^2/\sigma_{\bar{v}}^2)$ used in the smoother design, assuming linear phase detector. The dotted curves in the figure plot the two-sided normalized loop noise bandwidth as computed from Eq. (12). As may be inferred from the figure, the two measures of performance are equal within the limits of statistical errors. The minimum phase error variance (corresponding to $L = \infty$) varies over a range of about 0.3 to 1.4 for $(\sigma_a^2/\sigma_{\bar{v}}^2)$ between 1 to 100. It is also apparent from the figure the fact that the number of delays required has an inverse relation to $(\sigma_a^2/\sigma_{\bar{v}}^2)$ to achieve asymptotic smoother performance. In Fig. 5 is plotted the real loop noise bandwidth $2B_{Lp,S}$ as a function of normalized smoother delay (LT/τ_F), where τ_F is the time constant of the optimal filter. As is clear from the figure, the normalized value of delays required to achieve asymptotic smoother performance does not depend significantly upon $(\sigma_a^2/\sigma_{\bar{v}}^2)$.

Figures 6 and 7 plot the results similar to those of Figs. 4 and 5 respectively, when the actual process noise variance equals its design value, i.e., $\sigma^2_{a,S} = \sigma^2_a$. A comparison of these two sets of figures shows that the phase error variance can be at most 1.35 times more than for the case of $\sigma^2_{a,S} = 0$. For intermediate values of the noise variance, $0 < \sigma^2_{a,S} \leqslant \sigma^2_a$, the ratio would be smaller.

In Fig. 8, a comparison of smoother phase error variance is made for three different sampling periods T equal to 0.01, 0.1 and 1 s respectively. As is evident from the figure, whereas the optimum filter performance is dependent upon the sampling period, the asymptotic smoother performance depends only marginally on T. Thus the smoother in the most part compensates for any loss of optimality due to finite sampling period. This means that smaller T can be used with smoothing than with filtering only.

3. Smoother performance with nonlinear phase detector. Figures 9 and 10 present the simulation results for the case of $(\sigma_a{}^2 = \sigma_{\bar{v}}{}^2)$ corresponding to a two-sided noise bandwidth of the filter equal to 1 Hz. For this filter design and in the absence of the process noise $(\sigma^2_{a,S} = 0)$, the effect of nonlinearity is to degrade the normalized phase error variance $P_S(1,1)/\sigma_{\bar{v}}{}^2$ by at most a factor of 1.32 for $\sigma_{\bar{v}}{}^2 \leqslant 2.2$ (corresponding to the filter rms phase error of 27° for linear detector and 30° for nonlinear phase detector).

For the case of $\sigma^2_{a,S} = \sigma^2_a$, the normalized phase estimation error variance depends much more strongly on $\sigma_{\bar{v}}{}^2$. For $\sigma_{\bar{v}}{}^2 < 1.4$ (corresponding to rms phase error of 28.5 degrees at the phase detector output), the degradation is within a factor of 1.7 (2.3 dB). The degradation can be much higher for larger values of $\sigma_{\bar{v}}{}^2$.

From these simulations it may also be inferred that for $\sigma^2_{a,S} = 0$, and for the case of linear phase detector, the smoother provides an improvement of 5.6 dB over the filter. When the phase detector nonlinearity is taken into consideration, then for a range of 10 log $(1/\sigma^2_\phi) \geqslant 6$ dB, with σ^2_ϕ denoting the phase error variance of the PLL with linear phase detector, the smoother still provides an improvement of at least 5.1 dB over the filter. Note, however, that the filter performance can itself be degraded by as much as 1.5 dB due to phase detector nonlinearity. Since these results correspond to a fixed value of B_L, it may be concluded that with a smoother, the receiver can be operated with at least 3.5 dB smaller carrier power to noise spectral density ratio (P_c/N_0) when it is desired to have 0.1 or smaller value for the phase error variance.

For the case of $\sigma^2_{a,S} = \sigma^2_a$, it is observed that the effects of nonlinearity are more dominant resulting in a threshold behavior in the smoother phase error variance. However, for 10 log $(P_c/N_0\ B_L) \geqslant 7.5$ dB, the results in terms of smoother performance are close to those for the case of $\sigma^2_{a,S} = 0$.

V. Conclusions

The article has presented the performance of suboptimal filter and smoother for the phase and frequency estimation of a sinusoidal carrier under the presence of both the process noise and observation noise. The performance predicted on the basis of linear estimation theory is in close conformity with the corresponding results obtained with simulations, when the phase detector is assumed linear. Similar results are applicable when the phase detector nonlinearity is taken into account and the receiver is operating under high SNR conditions. Under these conditions the smoother improves both the phase and frequency estimation error compared to the filter by about 6 dB.

However, as the SNR is reduced, the corresponding improvement is less. Also the reduction is more when the process noise is present than when only the observation noise is present. Overall taking into account the degradation caused by the nonlinearity in the performance of filter, the smoother can permit the receiver operation at about 3.5 dB smaller carrier power to noise spectral density ratio when it is desired to have 0.1 or smaller value of the phase error variance.

Acknowledgment

The first author acknowledges a partial support provided by California State University in the form of a faculty research award.

References

1. D. C. Youla, "The Use of the Method of Maximum Likelihood in Estimating Continuous-Modulated Intelligence Which has been Corrupted by Noise," *IRE Trans. Inform. Theory, PGIT-3*, pp. 90–105, March 1954.

2. H. L. Van Trees, "Analog Communication Over Randomly-Time-Varying Channels," *IEEE Trans. Inform. Theory, IT-12*, pp. 51–63, January 1966.

3. A. J. Viterbi, "On the Minimum Mean Square Error Resulting from Linear Filtering of Stationary Signals in White Noise," *IEEE Trans. Inform. Theory, IT-11*, pp. 594-595, October 1965.

4. H. L. Van Trees, "Application of State-Variable Techniques in Detection Theory," *Proc. IEEE, 58*, pp. 653–669, May 1970.

5. D. L. Snyder, *The State Variable Approach to Analog Communication*. Cambridge, Mass.; MIT Press, 1971.

6. R. E. Kalman and R. S. Bucy, "New Results in Linear Filtering and Prediction Problems," *J. Basic Eng., Ser. D, Vol. 83*, pp. 95–108, March 1961.

7. C. N. Kelly and S. C. Gupta, "Discrete-Time Demodulation of Continuous-Time Signals," *IEEE Trans. Inform. Theory, IT-18*, pp. 448-493, July 1972.

8. A. M. Jazwinski, *Stochastic Processes and Filtering Theory*. Academic Press, New York: 1970.

9. S. Prasad and A. K. Mahalanabis, "Finite Lag Receivers for Analog Communication," *IEEE Trans. Comm., COM-23*, pp. 204-211, February 1975.

10. R. Kumar, *Optimum Filters and Smoothers Design for Carrier Phase and Frequency Tracking*, to appear as JPL Publication, Jet Propulsion Laboratory, Pasadena, Calif., 1987.

11. C. A. Pomalaza Raez and W. J. Hurd, "Improved Carrier Tracking by Smoothing Estimates," *IEEE Trans. Aerosp. Electron. Syst., AES-21*, pp. 610-618, September 1985.

12. B. Ekstrand, "Analytical Steady-State Solutions for Kalman Tracking Filter," *IEEE Trans. on Aerosp. Electron. Syst., 19*, pp. 815-819, November 1983.

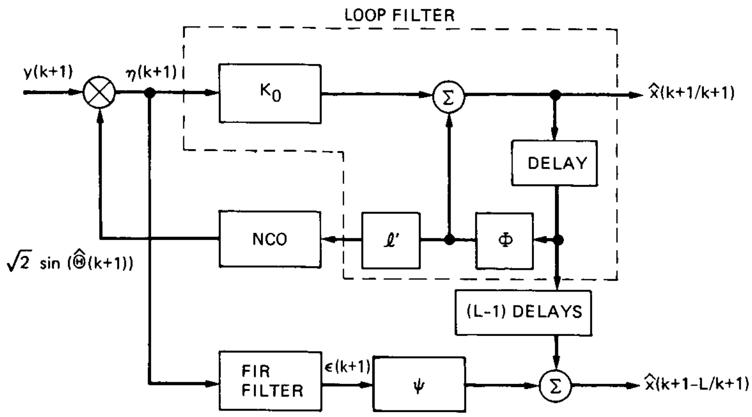

Fig. 1. An equivalent and simpler implementation of the smoother

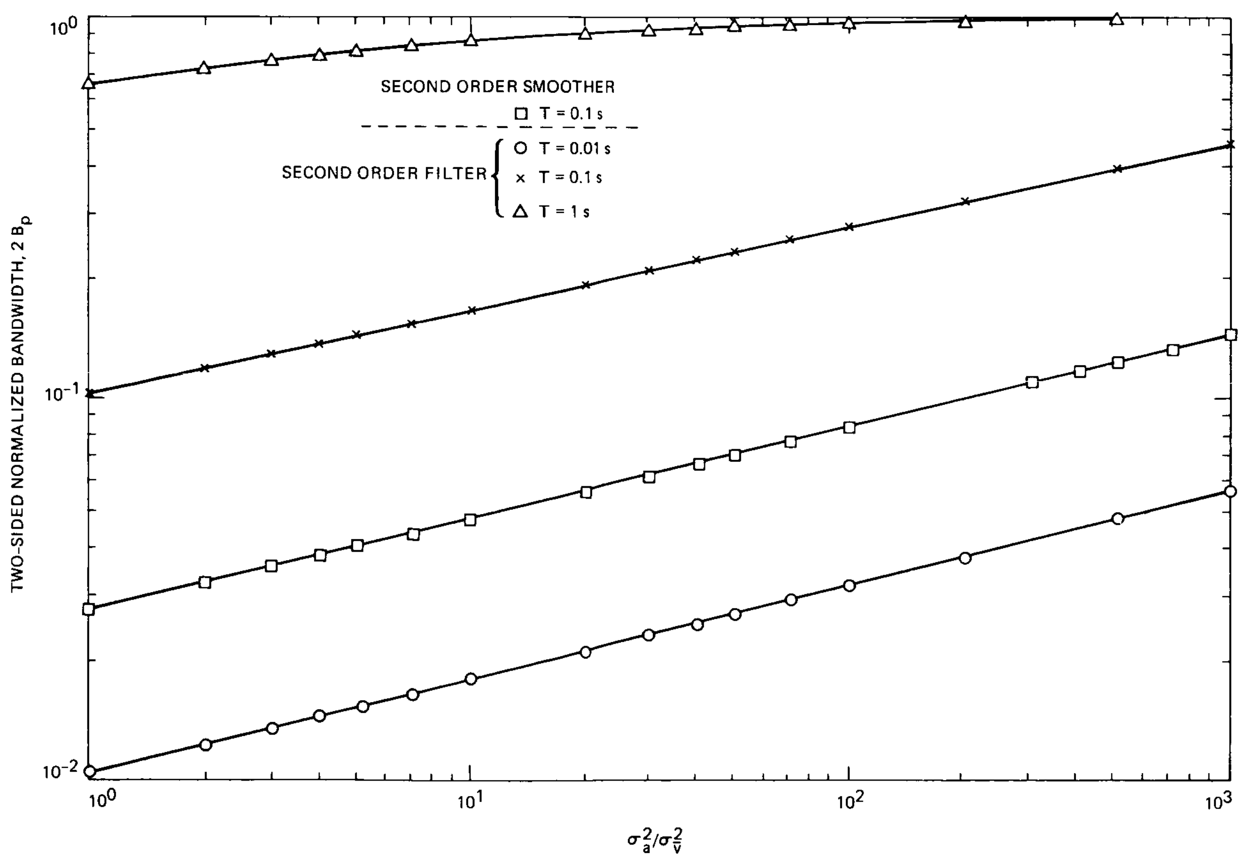

Fig. 2. Normalized loop noise bandwidth of the second order filter/smoother vs (σ_a^2/σ_v^2)

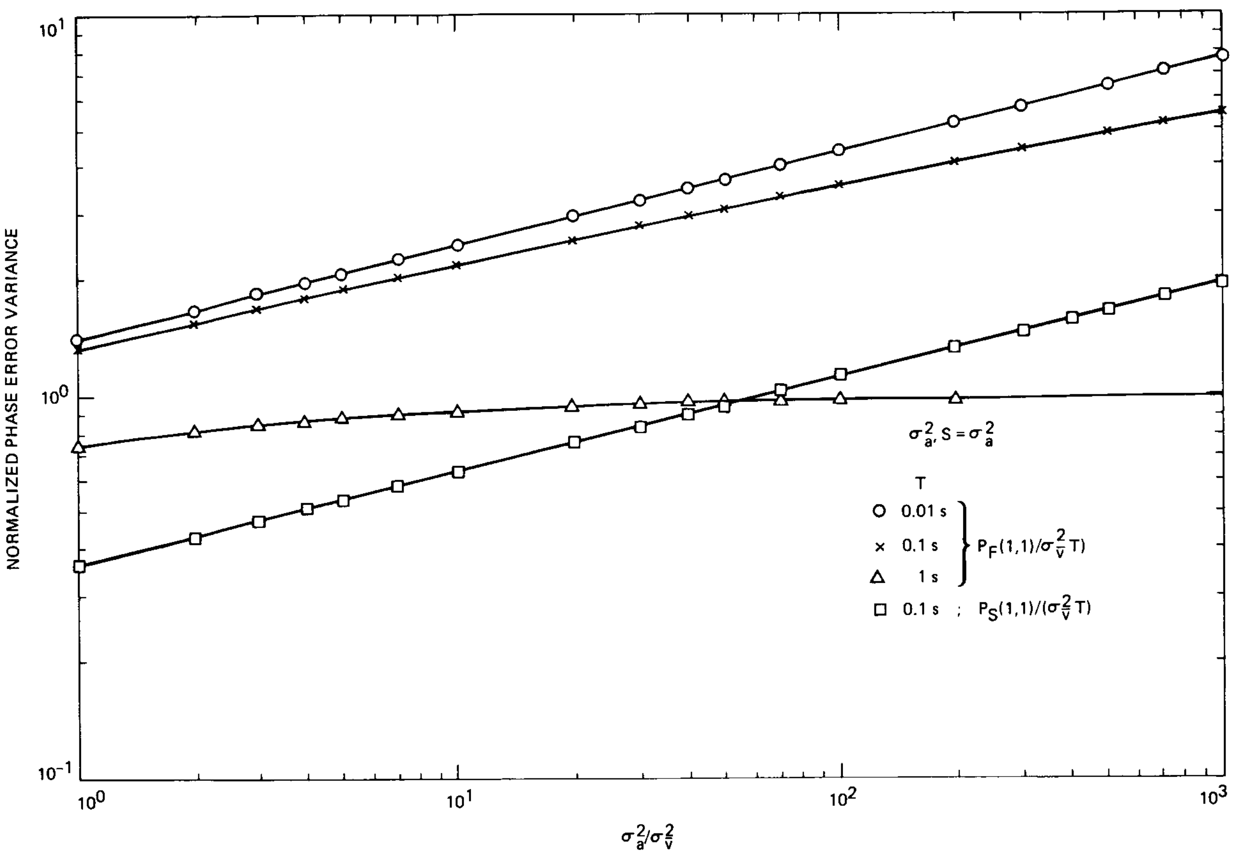

Fig. 3. Normalized phase error variance vs (σ_a^2/σ_v^2) with $\sigma_{a,S}^2 = \sigma_a^2$

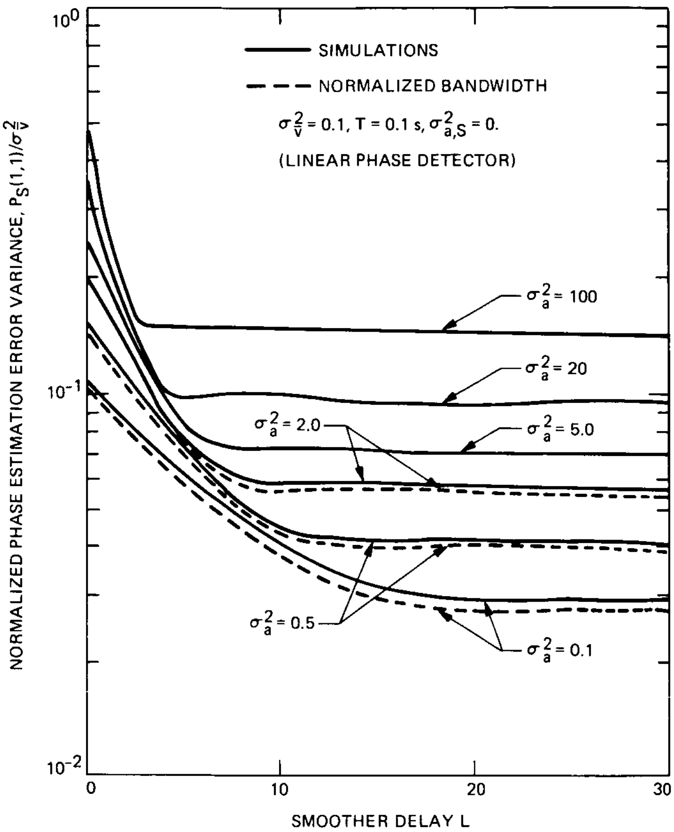

Fig. 4. Smoother estimation error variance vs smoother delay ($\sigma_{a,S}^2 = 0$)

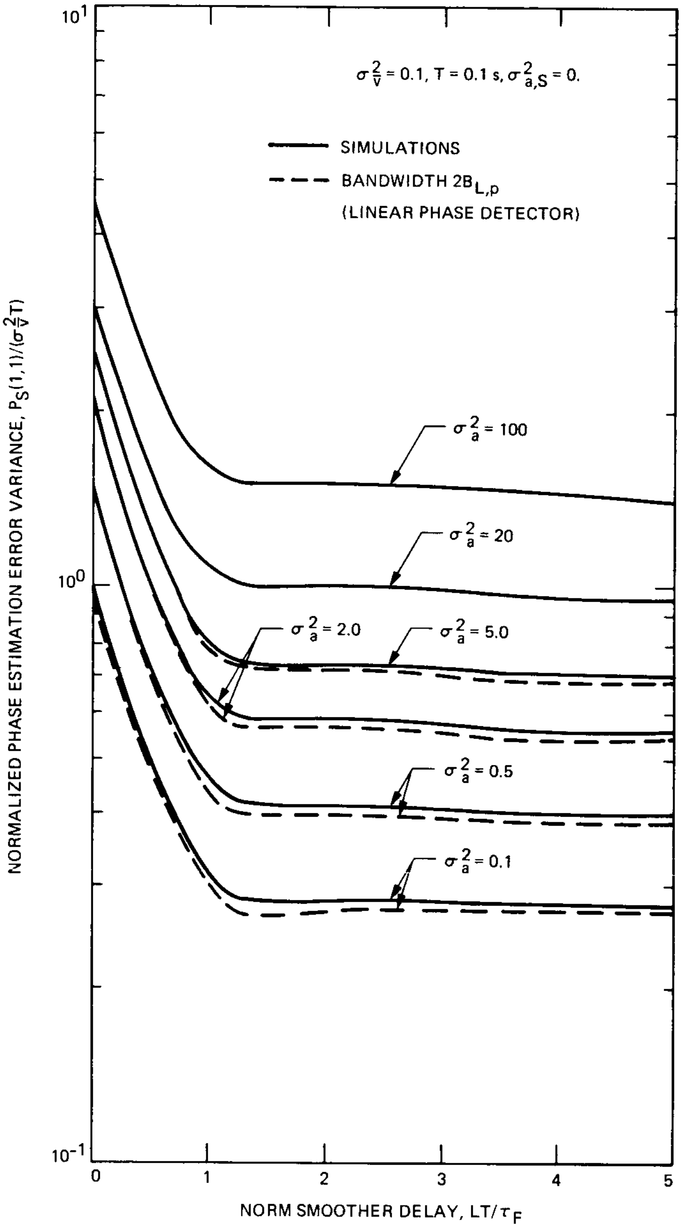

Fig. 5. Normalized smoother estimation error variance vs normalized delay ($\sigma_{a,S}^2 = 0$)

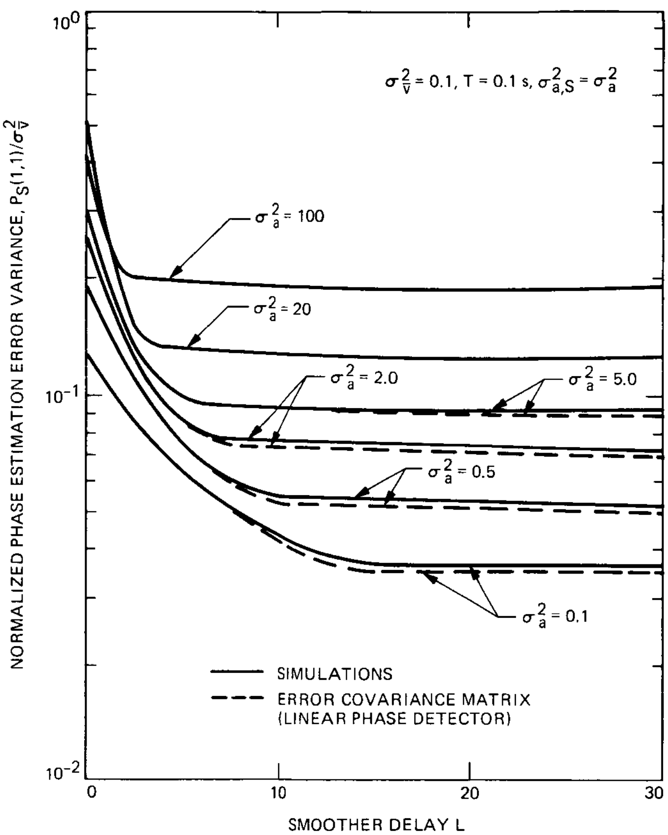

Fig. 6. Smoother estimation error variance vs smoother delay ($\sigma_{a,S}^2 = \sigma_a^2$)

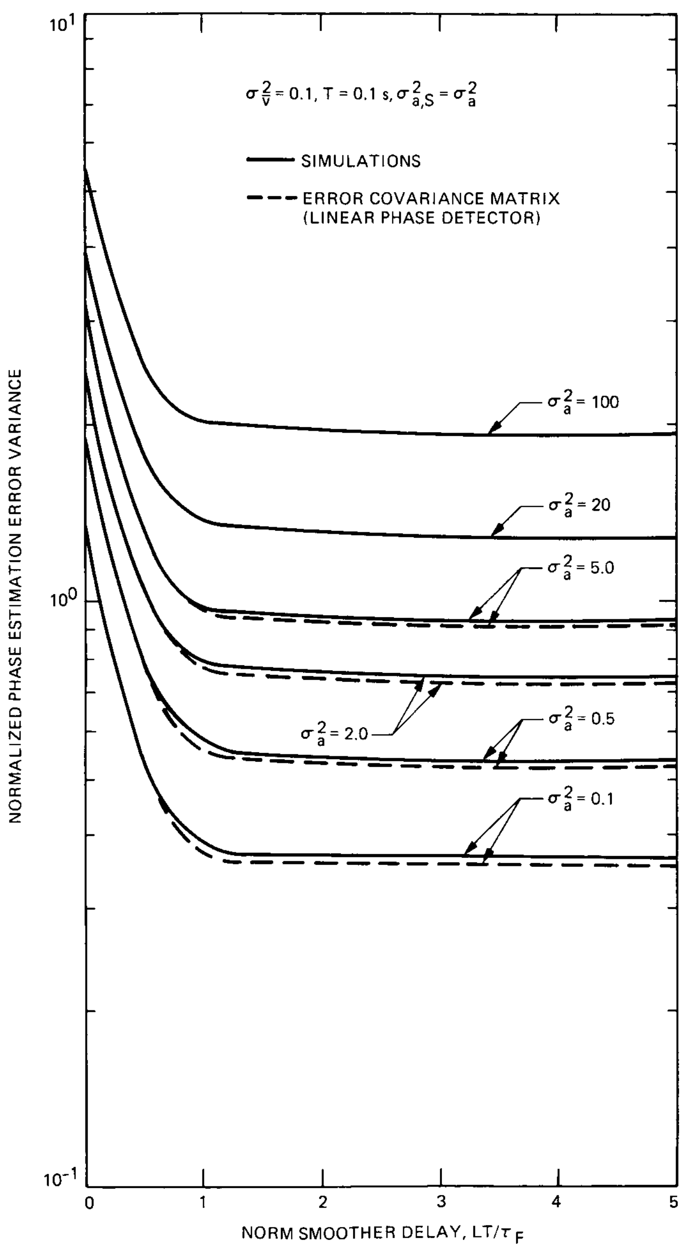

Fig. 7. Normalized smoother estimation error variance vs normalized delay ($\sigma_{a,S}^2 = \sigma_a^2$)

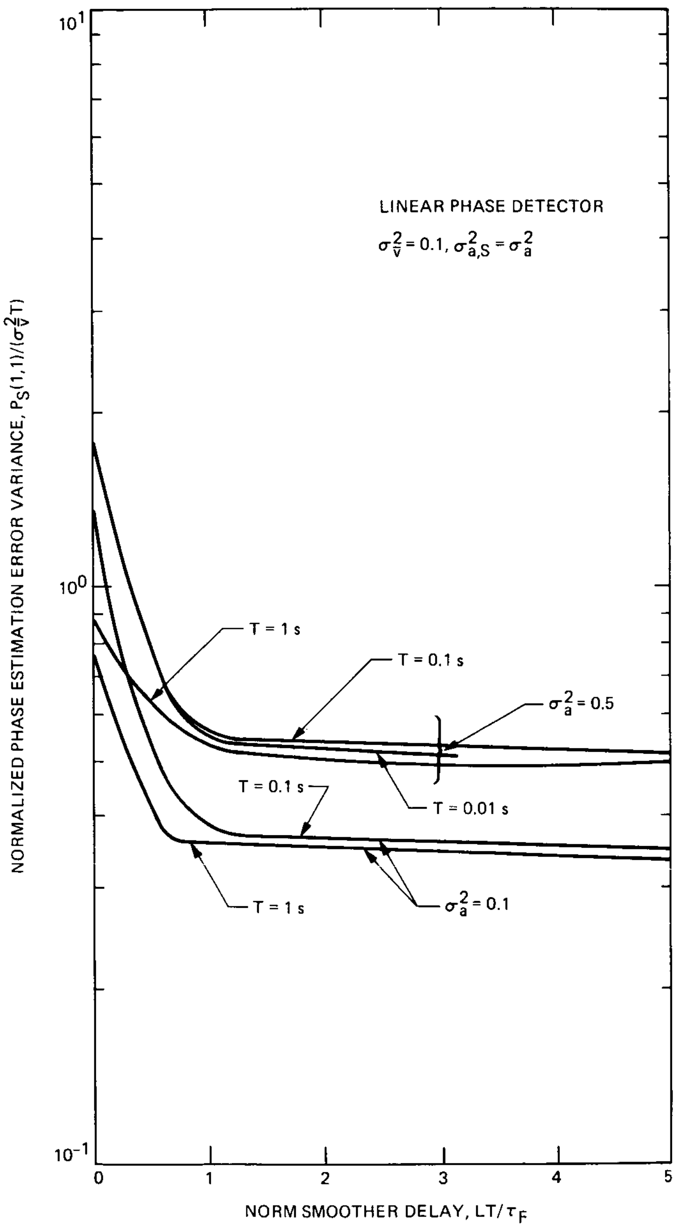

Fig. 8. Smoother performance for different sampling periods

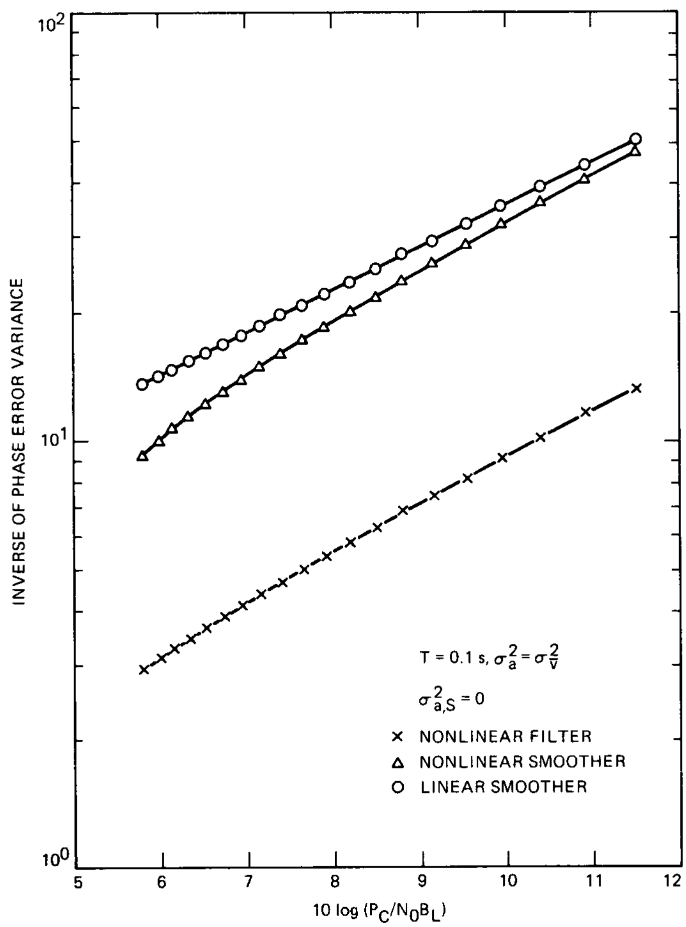

Fig. 9. Comparison of smoother performance with linear and nonlinear phase detectors ($\sigma_{a,S}^2 = 0$)

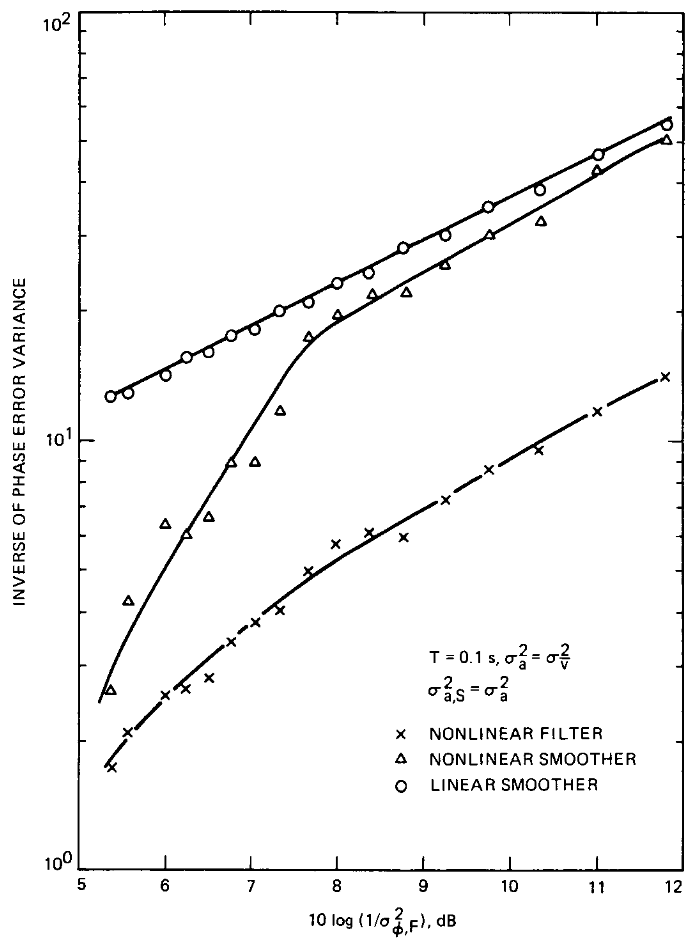

Fig. 10. Comparison of smoother performance with linear and nonlinear phase detectors ($\sigma^2_{a,S} \neq 0$)